

Inactivation of Ovine Cyclooxygenase-1 by Bromoaspirin and Aspirin: A Quantum Chemistry Description

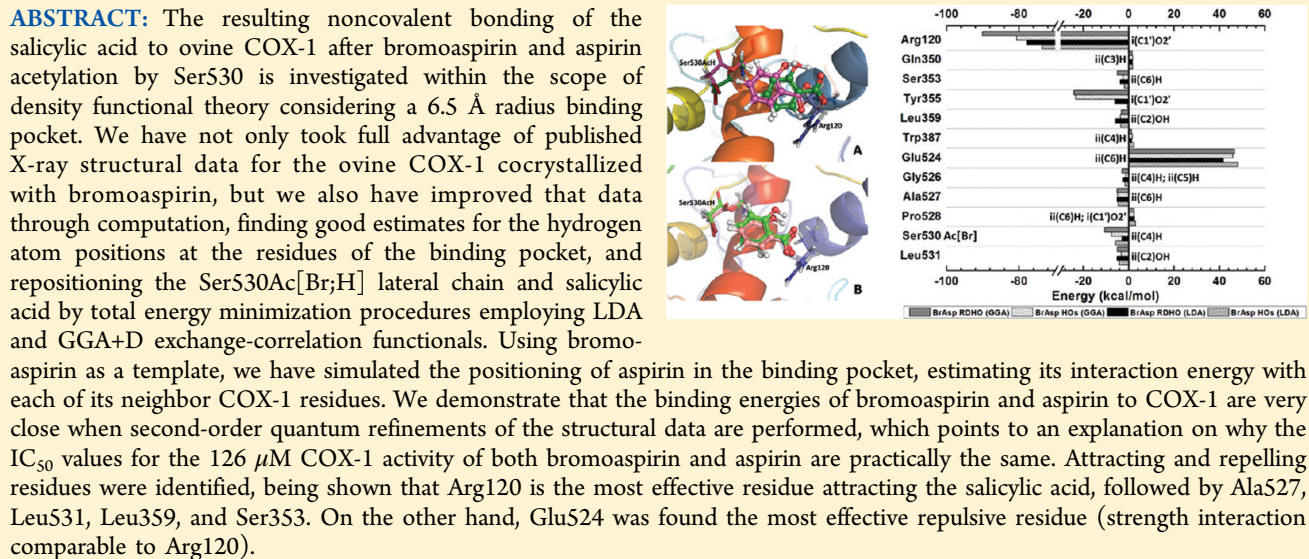
Ito L. Barroso-Neto,[†] João Paulo C. Marques,[‡] Roner F. da Costa,[‡] Ewerton W. S. Caetano,^{*,§} Benildo S. Cavada,[†] Carmem Gottfried,[†] and Valder N. Freire[‡]

[†]Department of Biochemistry, Universidade Federal do Ceará, Fortaleza 60455-760, Ceará, Brazil

[‡]Department of Physics, Universidade Federal do Ceará, Fortaleza 60455-760, Ceará, Brazil

[§]Instituto Federal de Educação, Ciência e Tecnologia do Ceará, Fortaleza 60040-531, Ceará, Brazil

[†]Department of Biochemistry, Universidade Federal do Rio Grande do Sul, Porto Alegre 90035-003, Rio Grande do Sul, Brazil



1. INTRODUCTION

After more than a century of clinical practice, aspirin remains a largely recommended antithrombotic, antipyretic, analgesic, and antiproliferative drug.^{1–3} It acts by blocking the biosynthesis of inflammatory prostanoid hormones through inhibition of cyclooxygenase enzymes (COXs), sterically hindering the entrance of the physiological binder arachidonic acid.⁴ Like other nonsteroidal anti-inflammatory drugs (NSAIDs) such as ibuprofen, diclofenac, ketoprofen, etc., aspirin inhibits—in different degrees—both COX-1 and COX-2 isoforms (note that a third distinct COX isozyme, COX-3, was described recently^{5,6}), being for the former 10–170 times more potent than for the latter.^{7–10} The available evidence suggests that the anti-inflammatory and analgesic properties of traditional NSAIDs are due to the inhibition of COX-2, whereas the ulcerogenic side effects of these inhibitors are associated with the blockage of COX-1.^{2–11} As a matter of fact, prolonged NSAIDs administration exhibit several undesired side effects, the most important being gastrointestinal irritation and ulceration, which still represent an unsolved therapeutic problem.^{11,12} COX-1 is constitutively expressed at high levels in cells and tissues such as endothelium, monocytes, platelets,

renal collecting tubules and seminal vesicles, indicating that it is developmentally regulated.¹³ Consequently, the COX-1 environment is neutral or slightly alkaline, with its pH between 7.2 and 7.4.

COX-1 was first purified in 1976,¹⁴ cloned in 1988,^{15–17} and cocrystallized with the analogue of aspirin, 2-bromoacetoxibenzoic acid (bromoaspirin), in 1995.¹⁸ COX-1 has 70 kDa, 22 kb gene size and chromosome 9q32-q33.3, with a 602 amino acids primary structure. It forms homodimers (see Figure 1) whose monomers are comprised of three structural domains: a N-terminal epidermal growth factor (EGF) domain, a membrane binding domain (MBD), and a large C-terminal catalytic domain, which comprises 80% of the protein and contains both the cyclooxygenase and peroxidase active sites.^{4,8} Each monomer contains a 25 Å hydrophobic channel that originates at the membrane binding domain and extends into the core of the globular domain.^{19–21} The COX-1 dimers are roughly ellipsoidal, and the structures of their monomers are

Received: July 6, 2011

Revised: February 2, 2012

Published: February 9, 2012

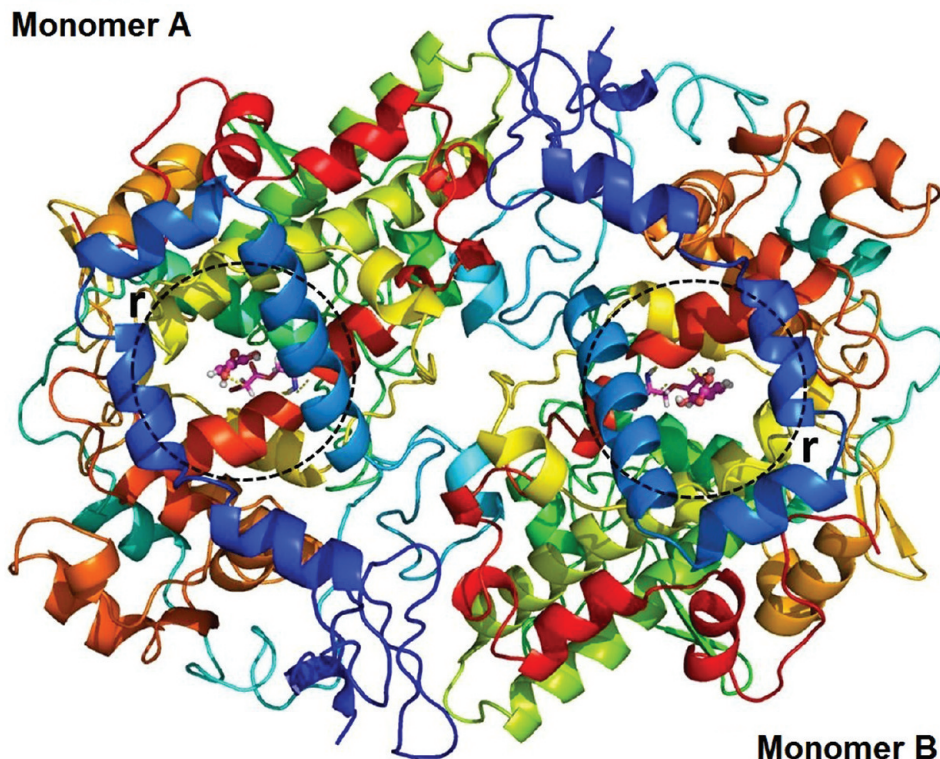


Figure 1. Ovine COX-1 dimer cocrystallized with bromoaspirin, PDB 1PTH. The residues belonging to the binding pockets are inside the dashed spheres of radius r around each bromoaspirin.

very similar. The dimer interface is relatively open, with numerous water molecules interspersed throughout. A total of twenty-two intermolecular polar interactions can be identified at the dimer interface as well as numerous hydrophobic interactions and bridging water molecules that contribute to the packing of the two monomers.

As a general rule derived from structural data, the NSAID binding site involves the upper half of this channel from Arg120 to near Tyr385, and several of these amino acids are uniquely important in cyclooxygenase catalysis.²² Amino acids lining the hydrophobic cyclooxygenase active site channel include Leu117, Arg120, Phe205, Phe209, Val344, Ile345, Tyr348, Val349, Leu352, Ser353, Tyr355, Leu359, Phe381, Leu384, Tyr385, Trp387, Phe518, Ile523, Gly526, Ala527, Ser530, Leu531, Gly533, and Leu534. Only three of the channel residues are polar (Arg120, Ser353, and Ser530). When aspirin binds to COX-1, it acetylates Ser530, while Arg120 binds to the carboxylate groups of fatty acids and to many NSAIDs.²²

Vane,²³ Ferreira,²⁴ and Smith and Willis²⁵ proposed that aspirin and other NSAIDs inhibit the enzyme activity that converts polyunsaturated fatty acids to prostaglandins during the inflammatory process. The structural basis of aspirin activity inferred from the crystal structure of inactivated prostaglandin H₂ synthase was unveiled by Loll, Picot, and Garavito.¹⁸ They have obtained a 3.4 Å resolution X-ray structure of the ovine COX-1 inactivated by the potent aspirin analogue bromoaspirin, which was used because the strong scattering power of the bromine atom allowed it to be unambiguously located even in a low resolution electron density map. The crystal structure of the bromoaspirin proved to be isosteric with that of aspirin,²⁶ being verified that aspirin inhibits COX-1 as efficiently as

bromoaspirin.¹⁸ According to the usual interpretation of the structural data, the most important residues in the aspirin-COX-1 binding pocket are Ser530, due to the irreversible aspirin acetylation; Arg120, which forms a salt bridge with the carboxylic acid moiety; and Ser353, due to its polar character. Besides, Ile523 is crucial since its mutation to Val523 transforms the first shell of the COX-1 active site to that of COX-2.

It should be noted that to determine which residues are most relevant in a drug-binding site interaction using only distances and bond lengths from X-ray structural data or docking procedures and classical molecular dynamics simulations²⁷ is somewhat limited. In particular, low resolution structural data can prevent a correct understanding of the role of residues and ligand atoms on the binding pocket features. A detailed picture of the aspirin pathway actions at the quantum level²⁸ of its bonding to COX-1 allows a quantitative estimate of the individual contributions to the total binding energy and should be very useful for the design of new aspirin derivatives. As emphasized by Zhou et al.,²⁹ quantum mechanical (QM) methods are becoming popular in computational drug design and development mainly because high accuracy is required to estimate (relative) binding affinities. According to Raha et al.,³⁰ the routine use of QM methods in all phases of *in silico* drug design is of upmost importance for the evolution of this field. QM methods can also be used locally to improve crystal structures.³¹ Nevertheless, the computational demands of a quantum refinement are very costly in comparison with standard crystal structure refinement, but as computers get faster and cheaper, it may become a standard tool.³¹

The purpose of this work is to present an improved description of the inactivation of COX-1 by bromoaspirin and aspirin through a quantum chemistry investigation of their

interaction with close residues inside the 6.5 Å radius region encircling the binding pocket. For the computations, the initial geometry of the protein–drug complex was obtained from the PDB 1PTH file containing the 3.4 Å resolution X-ray structure of the ovine COX-1 cocrystallized with bromoaspirin.¹⁸ We simulate the conversion of bromoaspirin into aspirin at the binding pocket by replacing Br with H in the acetylated Ser530 residue, Ser530Ac[Br;H]. The binding site is stabilized by a quantum mechanics based energy minimization procedure, allowing an improved positioning of drug, residue hydrogen atoms, and Ser530Ac[Br;H] lateral chains in comparison with the original structural data. Finally, the interaction energy between the COX-1 binding site and the theoretically adjusted molecule of salicylic acid is obtained by using the molecular fractionation with conjugate cap (MFCC) scheme (refs 37–40).

2. COMPUTATIONAL DETAILS

Quantum molecular simulation methods are frequently used to describe systems with tens up to thousands of atoms. Despite the complexity of biological systems, the rapidly increasing computational power in the past decade, combined with the improvement of quantum methods like density functional theory (DFT)^{32,33} has allowed the application of quantum mechanics (many times combined with molecular mechanics techniques) to study, for example, enzymatic reactions and the structure of proteins and their ligand binding sites.^{34–48} In particular, fragment-based methods for quantum calculations involving protein systems have been developed to speed up the calculations in these systems.^{49–58}

All geometry optimizations in this work were evaluated using the DMOL3 DFT code within both the local density approximation (LDA) and dispersion corrected generalized gradient approximation (GGA+D) for the exchange-correlation energy.^{59–61} It is well-known that pure DFT methods are not able to describe accurately systems where noncovalent bonding is important.^{62–65} Besides, LDA is not adequate to characterize hydrogen bonds. However, some reports show that the local density approximation (LDA) can be used to treat systems (graphite, guanine hydrated crystals, aromatic binding of ligands to an enzyme) where the noncovalent bonding is relevant.^{66–69} After these results, and due to the relatively cheap computational cost of LDA simulations, we have opted for this functional. Besides, in order to make a comparison with a more sophisticated method, we also have performed calculations using the semiempirical GGA+D exchange-correlation energy, which is able to take into account noncovalent forces such as hydrogen bonding and van der Waals interaction. The state of the art in semiempirical correction methods for dispersive forces is given by the Tkatchenko–Scheffler (TS) scheme,⁶¹ which accounts to some degree for the relative variation in dispersion parameters of differently bonded atoms.

A double numerical plus polarization (DNP) basis set was adopted to expand the Kohn–Sham orbitals together with DFT semicore pseudopotentials. The orbital cutoff was set to 3.7 Å, and a total energy variation smaller than 10⁻⁶ Ha was assumed to achieve self-consistency. For the geometry optimization, convergence tolerances were maximum energy variation smaller than 10⁻⁵ Ha, maximum force per atom smaller than 0.002 Ha/Å, and maximum atomic displacement smaller than 0.005 Å. After reaching convergence, the residue–drug interaction energies were obtained by capping the isolated residues following the molecular fractionation with conjugate caps (MFCC) scheme proposed by Zhang and Zhang.^{37–40}

A suitable choice of conjugated caps is crucial for the method to comply with the chemical valence requirements and mimic the local electronic environment of the original protein around the capped fragments.⁵⁸ In the MFCC computations, the interaction energy between the 2-benzoic acid molecule *M* and each amino acid residue *R_i*, *E*(*M* – *R_i*), was calculated according to

$$\begin{aligned} E(M - R_i) = & [E(M - C_i R_i C_i^*) - E(C_i R_i C_i^*)] \\ & - [E(M - C_i C_i^*) - E(C_i C_i^*)] \end{aligned} \quad (1)$$

The *C_i(C_i^{*})* cap is obtained by taking the residue neighbor *R_{i+1}* (*R_{i-1}*) and attaching a carboxyl (amine) group to its dangling bond (we convention here that the sequence of residues {R_i} is taken along the primary structure of the protein from the amine to the carboxyl tail). At the right side of eq 1, the first term *E*(*M* – *C_iR_iC_i^{*}*) is the total energy of the system formed by the 2-benzoic acid and the capped residue. The second term, *E*(*C_iR_iC_i^{*}*), gives the total energy of the capped residue alone, while the third term, *E*(*M* – *C_iC_i^{*}*), is the total energy of the system formed by the drug and the hydrogenated set of caps (hydrogen positions being optimized using DFT). Finally, *E*(*C_iC_i^{*}*) is the total energy of the system formed by the hydrogenated caps only.

In our calculations, only a COX-1 fragment formed from residues within a radius of 6.5 Å from the drug is taken into account for hydrogen atoms geometry optimization. The input data for the DFT calculations were obtained from the 3.4 Å resolution X-ray crystal structure of ovine COX-1 inactivated by the potent aspirin 2-bromoacetoxybenzoic acid (bromoaspirin) published by Joll et al.¹⁸ Figure 1 shows their published dimer structure, PDB entry 1PTH. For each monomer (A and B), we can build a sphere of radius *r* around bromoaspirin containing the relevant interacting residues. If *r* = 5 Å, there are 11 residues in the binding pocket interacting with bromoaspirin, while for *r* = 6.5 Å there are 19 residues. Because of the similarity of the binding pockets in the COX-1 dimer, the DFT calculations were performed for one monomer only.

The protonation state of the 2-benzoic acid depends on the pH condition and was taken into account in our calculations. As a matter of fact, considering a neutral or slightly alkaline environment (as in the blood and in the intracellular medium, pH 7.2–7.4), the salicylic acid becomes deprotonated, i.e., the hydrogen atom bounded to the carboxylic group is removed, and a negative charge (–e) is assigned to the oxygen atoms (see Figure 2).

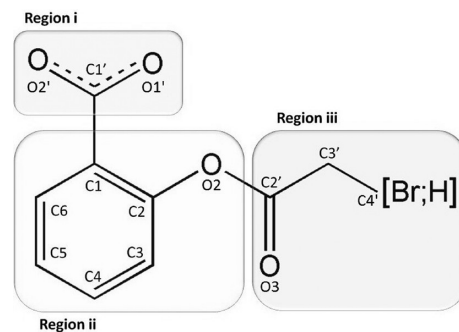


Figure 2. Bromoaspirin [see the C3'Br bond] and aspirin [see the C3'H bond] molecules. Three regions are distinguished: *i*, *ii*, and *iii*. They are usually found in a neutral or slightly alkaline environment, pH 7.2–7.4, giving rise to the protonation state in which a negative charge –e is assigned to the oxygen atoms (dashed line).

Therefore, one must consider the salicylic acid deprotonated state in any improved description of the COX-1 inactivation by bromoaspirin and aspirin. The pH related COO^- -charged state contributes significantly to the inactivation effectiveness of COX-1.

As mentioned before, the original crystal structure of ovine COX-1 used to carry out the computations has a covalently bounded bromoaspirin molecule as ligand. To overcome the lack of experimental data, we have added the hydrogen atoms of the system manually and have carried out a geometry optimization for the hydrogen atoms only, keeping the non-hydrogen species frozen. Structures optimized in this way will be called here hydrogen only optimized structures (HOs). An improvement over the HOs is to allow, besides the relaxation of the hydrogen atoms, for the relaxation of all non-hydrogen atoms of the drug, leading to a drug and hydrogen optimized structure (DHO). Finally, one can also allow the relaxation of the hydrogen atoms, drug and the non-hydrogen atoms of amino acid residues of interest at the binding pocket. This approach will lead to a residue–drug–hydrogen optimized structure (RDHO), being adopted here to include the relaxation of the acetylated Ser530 residue and to simulate the structure of an aspirin molecule at the same binding pocket, after replacing the bromine atom by hydrogen.

Initially, 11 residues, those within a radius of 5 Å from the 2-benzoic acid centroid, were selected to carry out the MFCC scheme: Val116, Arg120, Val349, Leu352, Ser353, Tyr355, Leu359, Ile523, Ala527, Ser530AcBr(H) (OAH530 in the PDB notation), and Leu531. However, since several residues of the structurally accepted COX-1 active site were missing in this selection, the binding pocket radius was extended to 6.5 Å, adding the following eight residues: Leu93, Gln350, Trp387, Phe518, Met522, Glu524, Gly526, and Pro528. We note that Leu93, Val116, Gln350, Met522, Glu524, and Pro528 are not considered as lining the hydrophobic COX-1 active site channel according to the usual interpretation of the COX-1 structural data.²²

3. RESULTS AND DISCUSSION

The 11 most important residues in the ovine COX-1 binding pocket interacting with the salicylic acid after bromoaspirin acetylation are shown in Figure 3A (DFT-LDA, HOs) and Figure 3B (DFT-LDA, RDHO). Figure 3C depicts the DFT-LDA simulated RDHO binding site for aspirin obtained after the Br → H replacement. As a general rule, the DFT RDHO results exhibit an average increase of about 0.48 Å (15%) for the distances between the binding pocket residues and the salicylic acid in comparison with the HOs optimized X-ray diffraction data (see Table 1 and Figure 4). Important structural changes for bromoaspirin occur for the distances to Trp387 (from 4.3 to 6.0 Å), Ser530AcBr (from 2.8 to 4.0 Å), Glu 524 (from 5.7 to 6.2 Å), and Pro528 (from 6.2 to 7.1 Å). The effect of these changes on the positioning of bromoaspirin in the binding pocket in the LDA case is shown clearly in Figures 5A and Figure 5C (for aspirin). The RDHO optimization increases the distance of the salicylic acid from Ser530AcBr. It is worth to remark that these distance changes (up to 2.0 Å) are smaller than the estimated resolution of 3.4 Å¹⁸ of the original diffraction data. More distances are given in Table 1 for the LDA data. On the other hand, the GGA+D functional predicts a smaller degree of structural variation for bromoaspirin (Figure 5B and Table 2), with an average distance increase of 0.40 Å (11%) of the RDHO

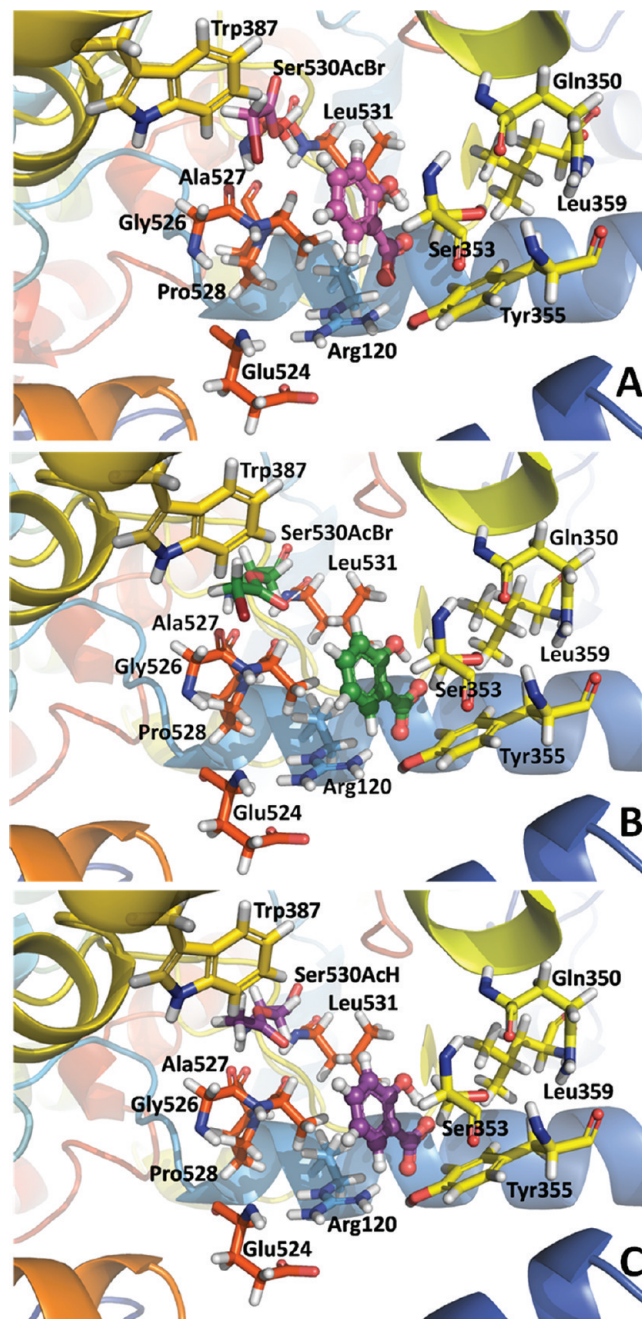


Figure 3. COX-1 binding pocket of bromoaspirin after Ser530 acetylation as obtained by DFT-LDA computations considering: (A) HOs geometry; (B) RDHO geometry; (C) a Br → H replacement (e.g., a bromoaspirin conversion to aspirin after Ser530 acetylation), RDHO geometry.

values with respect to the HOs data. All in all, the DFT-based refinement of structural data can be useful to provide a more accurate description of the active COX-1 binding site, a result which should also be valid for the active sites of proteins in general.³¹

The Binding Energy Panel BIRD. In order to map visually the MFCC interaction energies, we present, in Figure 6, a binding site, interaction energy, and residues domain (BIRD⁷⁰) panel for bromoaspirin and the 11 most important residues of the COX-1 binding pocket. The BIRD panel depicts, in a concise way, (i) the interaction energy (in kcal/mol) of a residue with which the drug interacts using horizontal bars,

Table 1. LDA Interaction Energies and Distances between the 19 Residues in the 6.5 Å COX-1 Binding Pocket and the Salicylic Acid after Ser530 Acetylation of Bromoaspirin and Aspirin^a

residue	group	BrAsp HOs		Asp RDHO		BrAsp RDHO	
		E (kcal/mol)	d (Å)	E (kcal/mol)	d (Å)	E (kcal/mol)	d (Å)
Leu93	i(C1')O2'	0.77	5.19	-0.42	4.53	-0.40	4.54
Val116	i(C1')O1'	-0.36	3.23	-6.64	2.09	-6.57	2.11
Arg120	i(C1')O2'	-73.59	2.59	-78.31	2.81	-77.80	2.82
Val349	ii(C2)OH; ii(C3)H	0.66	2.23; 2.30	-1.66	2.52; 2.40	-1.73	2.48; 2.42
Gln350	ii(C3)H	1.83	6.16	1.63	6.40	1.63	6.43
Leu352	ii(C4)H	-0.49	2.45	-0.80	4.23	-0.84	4.22
Ser353	ii(C6)H	-1.85	3.89	-3.59	4.34	-3.66	4.28
Tyr355	i(C1')O2'	-0.56	2.74	-6.07	3.71	-6.09	3.70
Leu359	ii(C2)OH	-3.47	4.07	-5.98	3.54	-5.89	3.58
Trp387	ii(C4)H	2.24	4.34	1.41	5.98	1.41	5.96
Phe518	ii(C5)H	0.07	3.52	-0.18	5.53	-0.19	5.51
Met522	ii(C5)H	-0.25	5.21	-1.41	5.78	-1.40	5.81
Ile523	ii(C5)H; ii(C6)H	0.53	2.53; 2.41	0.41	2.13; 4.20	0.41	2.07; 4.19
Glu524	ii(C6)H	48.02	5.66	41.64	6.27	41.65	6.30
Gly526	ii(C4)H; ii(C5)H	-1.57	5.66 ; 5.47	-2.62	5.66; 6.30	-2.63	5.67; 6.36
Ala527	ii(C6)H	-4.55	2.75	-5.03	3.12	-5.12	3.14
Pro528	ii(C6)H; i(C1')O2'	2.98	6.17; 6.24	2.52	6.25; 7.09	2.51	6.30; 7.09
Ser530 Ac[H; Br]	ii(C4)H	-5.88	2.80	0.29	4.82	-2.97	3.90
Leu531	ii(C2)OH	-4.24	2.43	-5.39	2.20	-5.13	2.22

^aThey were calculated considering the HOs and RDHO DFT optimization levels of the original crystal diffraction data as published in the PDB 1PTH.

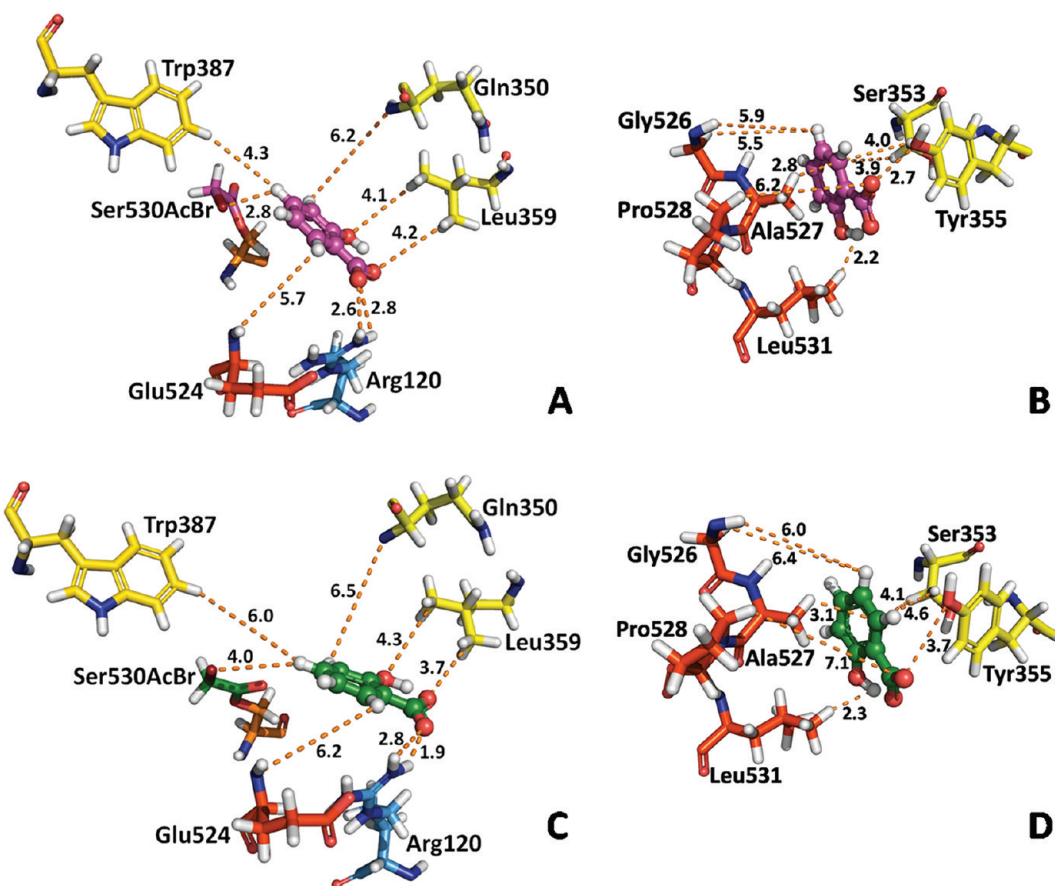


Figure 4. Distances in Å (small numbers) between the 11 most important residues in the COX-1 binding pocket of bromoaspirin after Ser530 acetylation as obtained by DFT-LDA: (A, B) HOs results; (C, D) RDHO data.

from which one can assign quantitatively the relevance of each residue at the binding site, whether attracting (negative energy)

or repelling (positive energy) the drug; (ii) the labels of the most important residues contributing to the binding, shown in

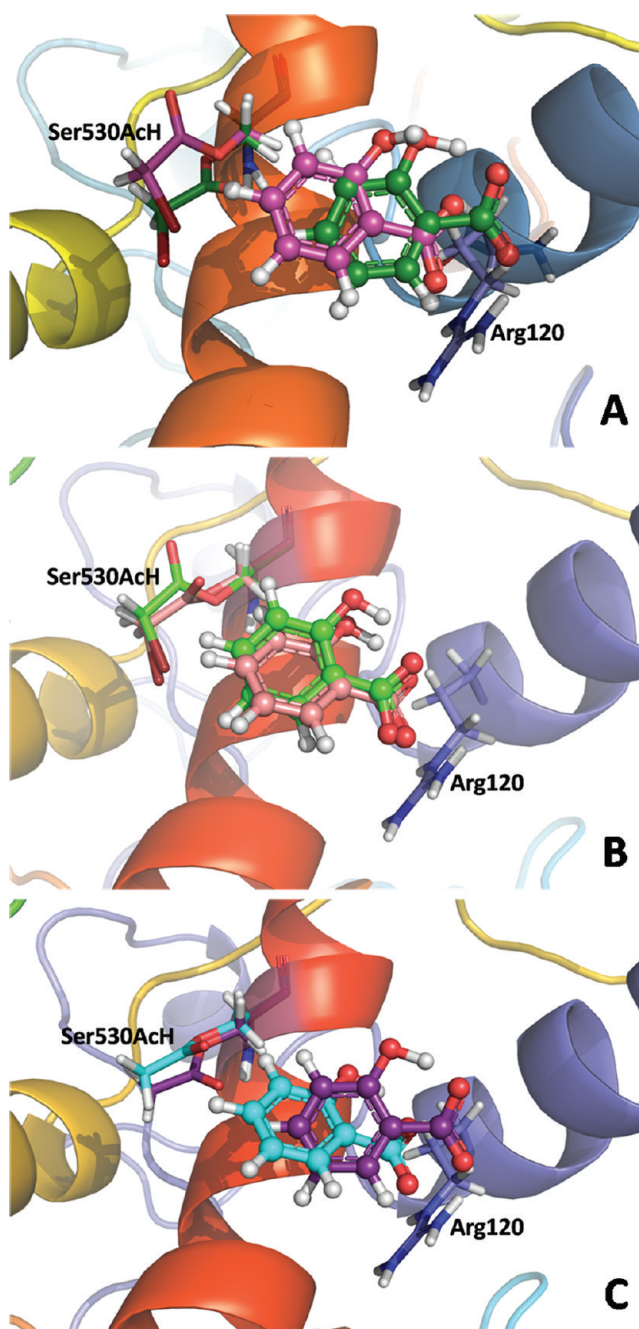


Figure 5. Salicylic acid positioning in the COX-1 binding site obtained after the HOs and RDHO DFT optimizations of the original structural data for bromoaspirin after Ser530 acetylation: (A) DFT-LDA HOs (magenta bonds/atoms) and RDHO (dark green) for bromoaspirin; (B) DFT-GGA+D HOs (light green) and RDHO (salmon) for bromoaspirin; (C) DFT-LDA HOs (cyan) and RDHO (purple) for aspirin.

a column at the left side; and (iii) the region of the drug (e.g., $i(C1')O$) which is closer to each residue of the binding site, placed at the side of the corresponding horizontal bar.

Arg120 and Glu524 are shown in Figure 6 to be the most important residues interacting with the salicylic acid after bromoaspirin acetylation, the former being attracted by the $i(C1')O_2'$ group with a HOs binding energy (defined here as the negative of the interaction energy) of 74 kcal/mol (78 kcal/mol, RDHO) in the LDA case and 81 kcal/mol (90 kcal/mol, RDHO) in the GGA+D case. For the Glu524 residue, the drug

$ii(C6)H$ region is repelled with a repulsive interaction energy of 48 kcal/mol (42 kcal/mol) in the case of HOs (RDHO) LDA optimization. The GGA+D corresponding figures are 46 kcal/mol (HOs) and 47 kcal/mol (RDHO). Ala527, Leu531, and Leu359 are attracting residues, interacting in this sequence with $ii(C6)H$, $ii(C2)OH$, and $ii(C2)OH$ with LDA HOs binding energies of 4.5, 4.2, and 3.5 (5.1, 5.1, and 5.9, RDHO) kcal/mol, and GGA+D binding energies of 4.8, 3.2, and 3.6 (5.1, 4.9, and 3.3, RDHO) kcal/mol, in respective order. Besides, Pro528, Trp387, and Gln350 are also repelling residues for the salicylic acid after bromoaspirin acetylation, interacting with $i(C1')O_2'$, $ii(C4)H$, and $ii(C3)H$ with repulsive HOs interaction energies of 3.0, 2.2, and 1.8 (2.5, 1.4 and 1.6, RDHO) kcal/mol, respectively, at the LDA level, and 2.4, 1.7, and 1.8 (2.3, 1.3, and 1.5, RDHO) at the GGA+D level. As a matter of fact, the total LDA (GGA+D) binding energy of bromoaspirin binding to COX-1 is 70 (100) kcal/mol using the RDHO optimization and 40 (79) kcal/mol considering the HOs level of calculation. The larger binding energy values for the first is a consequence of the improved positioning for the salicylic acid and residues in the ovine COX-1 binding pocket after the relaxation of the hydrogens, drug, and acetylated Ser530 in the RDHO approach.

The BIRD panel of Figure 7 shows the MFCC interaction energies for aspirin in comparison with bromoaspirin after the Ser530 acetylation using the RDHO optimization. After adding up all the MFCC interaction energies after aspirin and bromoaspirin acetylation, we obtain that the total LDA (GGA+D) binding energy of bromoaspirin and aspirin are close, being 73 (108) kcal/mol for the former and 70 (100) kcal/mol for the latter. This result is consistent with the identical IC_{50} values for the 126 μM COX-1 activity of both bromoaspirin and aspirin.¹⁸ We note that this conclusion is possible only because structural data for aspirin after Ser530 acetylation were obtained computationally within the DFT framework. Once more, as occurred for bromoaspirin, Arg120 and Glu524 are shown to be the most important residues interacting with the salicylic acid, now after aspirin acetylation, with a LDA (GGA+D) binding energy of 78 (90) kcal/mol for the first (again attracted by the $i(C1')O_2'$ group, a stronger binding in comparison with bromoaspirin) and a repulsive interaction energy of 42 (47) kcal/mol for the latter (repelled by the $ii(C6)H$ group, a bit weaker than observed for the bromine variant). Ala527, Leu531, and Leu359 appear again interacting with $ii(C6)H$, $ii(C2)OH$, and $ii(C2)OH$ with LDA (GGA+D) binding energies of 5.0 (5.1), 5.4 (4.9), and 6.0 (3.2) kcal/mol, respectively, while Pro528, Trp387, and Gln350 remain as repulsive residues for the salicylic acid after aspirin acetylation, interacting with $i(C1')O_2'$, $ii(C4)H$, and $ii(C3)H$ with positive LDA (GGA+D) interaction energies: 2.5 (2.3), 1.4 (1.3), and 1.6 (1.5) kcal/mol, in this order. Our results reinforce the structural results pointing to the importance of the Arg120 residue for the binding of aspirin to COX-1. Tables 1 (LDA) and 2 (GGA+D) summarize the data obtained for the interaction energies and drug–residue distances for bromoaspirin and aspirin.

DFT-LDA (DFT-GGA+D) calculated electrostatic potential isosurfaces around the salicylic acid and the most attractive and repelling residues of bromoaspirin and aspirin after Ser530 acetylation are shown in Figure 8A (8C) and Figure 8B (8D), respectively. The total electron density was projected onto them, revealing a negative charge density in the COO^- region (as expected due to the deprotonation). Since Arg120 has

Table 2. GGA+D Interaction Energies and Distances between the 19 Residues in the 6.5 Å COX-1 Binding Pocket and the Salicylic Acid after Ser530 Acetylation of Bromoaspirin and Aspirin^a

residue	group	BrAsp HOs		Asp RDHO		BrAsp RDHO	
		E (kcal/mol)	d (Å)	E (kcal/mol)	d (Å)	E (kcal/mol)	d (Å)
Leu93	i(C1')O2'	0.24	5.20	-0.23	4.81	-0.23	4.82
Val116	i(C1')O1'	-1.08	3.23	-1.29	3.55	-1.29	3.55
Arg120	i(C1')O2'	-80.58	2.45	-89.92	2.22	-90.04	2.22
Val349	ii(C2)OH; ii(C3)H	3.25	2.20; 2.22	-3.26	3.30; 2.98	-3.19	3.29; 2.92
Gln350	ii(C3)H	1.76	6.16	1.55	7.02	1.54	6.96
Leu352	ii(C4)H	-1.78	2.38	-2.88	2.51	-2.86	2.49
Ser353	ii(C6)H	-2.44	3.94	-4.91	2.95	-4.91	2.96
Tyr355	i(C1')O2'	-23.23	1.74	-24.18	1.59	-24.15	1.59
Leu359	ii(C2)OH	-3.58	4.05	-3.24	5.27	-3.25	5.26
Trp387	ii(C4)H	1.72	4.29	1.28	4.50	1.28	4.51
Phe518	ii(C5)H	-0.50	3.51	-0.79	3.76	-0.77	3.77
Met522	ii(C5)H	-3.36	5.21	-3.61	6.34	-3.58	6.37
Ile523	ii(C5)H; ii(C6)H	-1.11	2.53; 2.47	-2.26	2.33; 2.81	-2.22	2.37; 2.81
Glu524	ii(C6)H	45.92	5.68	46.65	6.47	46.65	6.47
Gly526	ii(C4)H; ii(C5)H	-1.40	5.67; 5.50	-2.97	5.87; 6.88	-2.96	5.90; 6.90
Ala527	ii(C6)H	-4.78	2.67	-5.06	3.31	-5.08	3.31
Pro528	ii(C6)H; i(C1')O2'	2.37	6.11; 6.22	2.33	7.10; 6.43	2.33	7.09; 6.43
Ser530 Ac[Br]	ii(C4)H	-7.60	2.78	-2.39	4.38	-10.54	3.44
Leu531	ii(C2)OH	-3.20	2.48	-4.87	2.61	-4.91	2.58

^aThey were calculated considering the HOs and RDHO DFT optimization levels of the original crystal diffraction data as published in the PDB 1PTH.

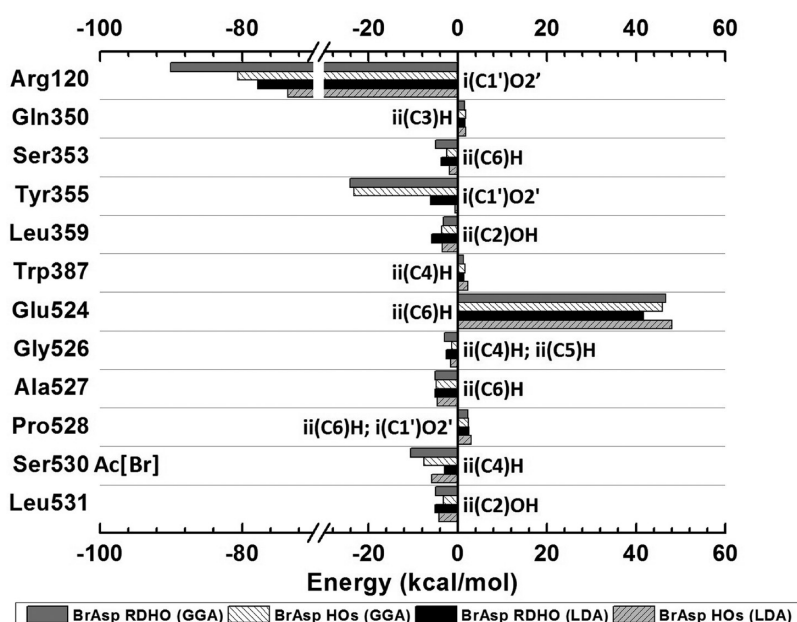


Figure 6. Interaction energy of the main COX-1 residues in the binding pocket of the monomer with the salicylic acid after Ser530 acetylation of bromoaspirin as obtained by DFT-LDA and DFT-GGA+D computations considering the HOs and RDHO geometry optimizations of the original structural data. The total LDA (GGA+D) bromoaspirin binding energies after Ser530 acetylation are 39.56 kcal/mol (79.37) and 70.21 (100.06) kcal/mol for the HOs and RDHO optimizations, respectively.

positive charge density and is closer to the COO^- group of the salicylic acid, one can conclude that the strong binding to this residue has a significant electrostatic component. On the other hand, Glu524 has a negatively charged oxygen near the COO^- group, which must contribute significantly to the repulsive character of its interaction with aspirin.

Usually, the determination of the main residues involved in the binding of a ligand is not an easy task. On the basis of structural data, the COX-1 active site is considered to have about 24 residues,²² from which it is currently accepted that

the polar residues Arg120, Ser353, and Ser530 are the most important. Besides, Ile523 and Tyr385 are important due to their mutation to Val523 and Phe385, respectively, which considerably reduces aspirin action.^{22,71} On the other hand, our results indicate that Leu359, Ala 527, and Leu531 bind the salicylic acid more strongly than Ser353 and Ser530. Consequently, the usual interpretation of the role of these residues must be reevaluated. By the way, Leu117, Phe205, Phe209, Val344, Ile345, Tyr348, Phe381, Leu384, Tyr385, Gly355, and Leu354 are outside the 6.5 Å binding pocket

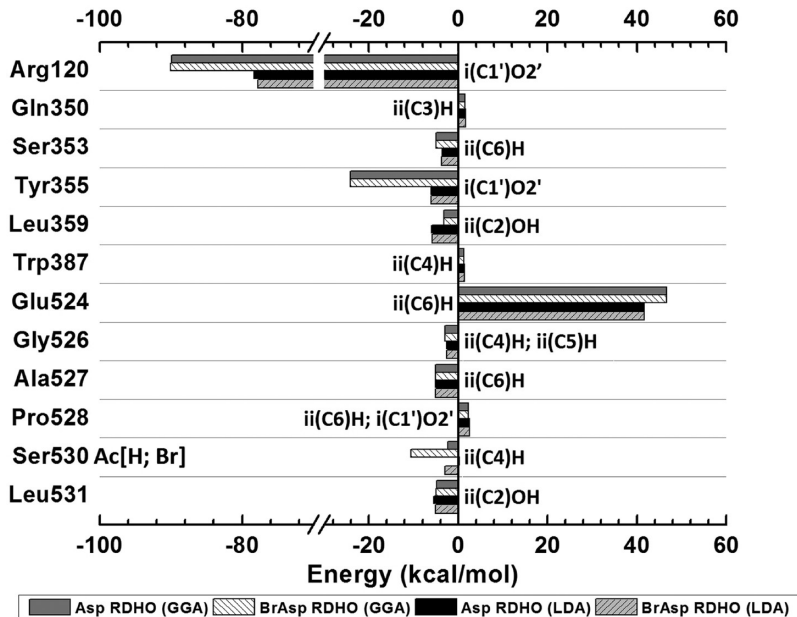


Figure 7. Interaction energy of the main COX-1 residues in the binding pocket of the monomer with the salicylic acid after Ser530 acetylation of aspirin as obtained by LDA and GGA+D DFT computations considering the RDHO optimization of the original structural data. The total LDA (GGA+D) aspirin binding energy after Ser530 acetylation is 72.82 (108.16) kcal/mol. For the sake of comparison, we also present similar data for the interaction energy of the main COX-1 with bromoaspirin. The total LDA (GGA+D) bromoaspirin binding energy after Ser530 acetylation is 70.21 (100.06) kcal/mol.

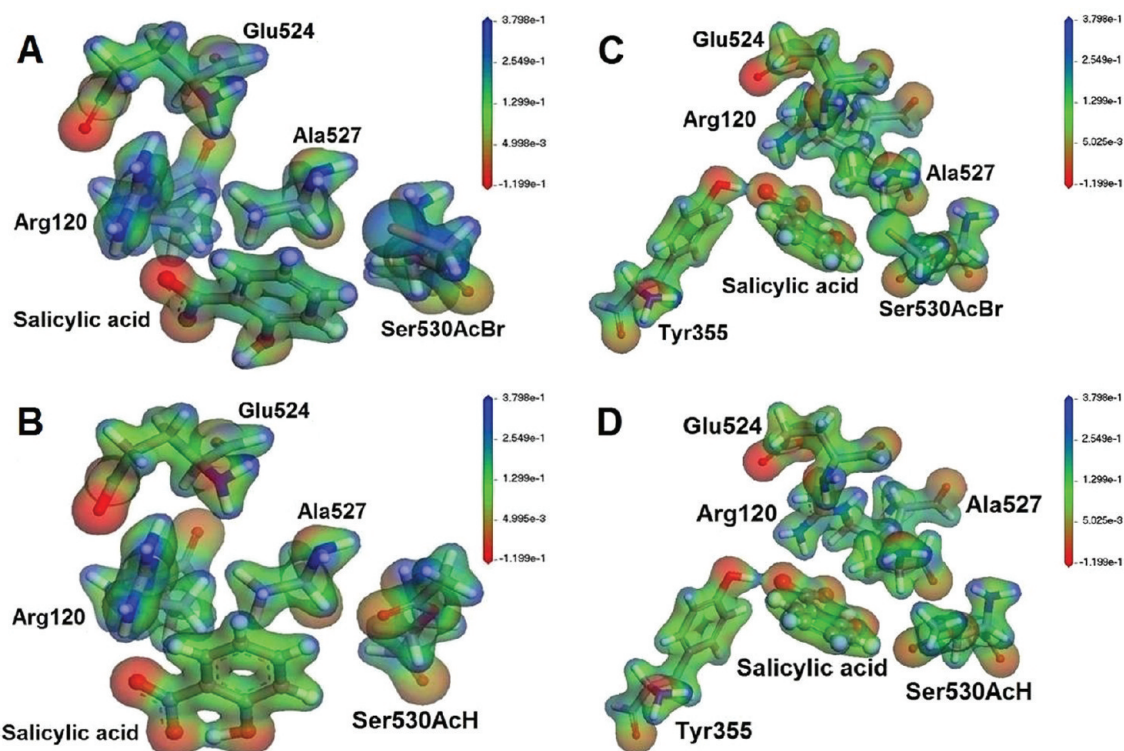


Figure 8. Electrostatic potential isosurfaces around the salicylic acid and the most attractive and repelling residues of bromoaspirin (A, C) and aspirin (B, D) after Ser530 acetylation as obtained by DFT-LDA (A, B) and DFT-GGA+D (C, D) computations considering RDHO optimized structure.

region of our focused ovine COX-1. Because of their larger distance to the salicylic acid, their individual interaction energies can be expected to be of the order of 1.0 kcal/mol, contributing by a little amount to the salicylic acid binding. On the other hand, Leu93, Val116, Gln350, Met522, Glu524, and Pro528 are residues inside the 6.5 Å binding pocket but were

not considered as important to the salicylic acid binding according previous interpretations based strictly on the structural data.²² Glu524, however, has a very strong repulsive (41.6 kcal/mol) interaction energy with the salicylic acid, which surely place it as the second most important residue for bromoaspirin and aspirin binding to COX-1.

With respect to the mutation related residues Ile523 and Tyr385, we have performed DFT-LDA calculations of their interaction energies with salicylic acid, finding energy values of 0.41 and 1.17 kcal/mol, respectively. We note that Tyr385 is outside the 6.5 Å binding pocket sphere, and its interaction energy was calculated for the sake of completeness, being stronger than the value for Ile523 (which is closer to the salicylic acid) due to its charge state. Consequently, the structural modifications related to the mutations Phe385 and Val523 can enhance locally their binding character. We highlight that our work suggest for the drug expert design some aspirin sites to be modified for the enhancement or decrease of its interaction with COX-1, ii(C3)H for example. Indeed, aspirin analogues with modifications at ii(C3)H have been proposed recently.⁷²

To assess the strength of van der Waals and electrostatic interactions, we also have performed DFT-GGA calculations for the most important residues, Arg120, Tyr355, and Glu524, removing the empirical dispersion correction (keeping a pure GGA functional) and including dispersion but keeping the BrAsp HOs molecule neutral. For Arg120, removing dispersion corrections increased its interaction energy by 1.8 kcal/mol, only, while removing the electrostatic effect increases the total energy by more than 60 kcal/mol. For Tyr355, the interaction energy increases from -23.23 to -21.77 kcal/mol when removing van der Waals contributions and to -17.21 kcal/mol when the electrostatic interaction is ignored. Finally, Glu524 becomes a bit more repulsive to the drug (interaction energy changes to 46.10 kcal/mol from 45.92 kcal/mol) if one suppresses dispersive forces and becomes attractive (interaction energy of -22.20 kcal/mol) if the electric charge of the BrAsp HOs molecule is neglected in the calculations. Overall, the electrostatic interaction is much more dominant than van der Waals for the main amino acid residues involved in the binding of BrAsp to COX-1.

4. CONCLUSION

Our results indicate that the use of docking procedures based solely on geometrical aspects can benefit significantly from quantum DFT computations for a clear evaluation of what are the main residues involved in the COX-1 inactivation by bromoaspirin and aspirin. Our interpretation of the experimental data after a DFT partial geometry optimization suggest the most important residues binding bromoaspirin and aspirin to COX-1 after acetylation are determined by a balance between charge state and distance to the salicylic acid. As a matter of fact, Arg120 is the most important attracting binding residue, being at a distance of 2.6–2.8 Å from i(C1')O1' and Glu524 is an important repulsive residue, despite being 5.7–6.2 Å distant from the drug, mainly due to its negative charge.

In summary, the first detailed quantitative evaluation of the role of 19 binding pocket residues on the inactivation of ovine COX-1 by bromoaspirin and aspirin was performed using quantum DFT calculations within the LDA and GGA+D approximations. Our results show that the LDA figures are in agreement with the more sophisticated GGA+D methodology, with the latter predicting larger values for the total binding energy of the drug–protein system. The simulations here presented give a practical demonstration that the quantum refinement of X-ray structural data can be consistently undertaken using approximations, contributing significantly for an improved understanding of experimental data. It is important to remark that previous structural based results

pointing Arg120 as the most effective residue attracting the salicylic acid after Ser530 acetylation were confirmed, while Glu524 was shown surprisingly to be very repulsive and the second most important effective residue at the binding site. We believe our results are very helpful in the understanding of COX-1 mutations on aspirin binding as well as for expert design of new aspirin derivatives.

■ AUTHOR INFORMATION

Corresponding Author

*Fax: +55-85-33073711; E-mail: ewcaetano@gmail.com.

Notes

The authors declare no competing financial interest.

■ ACKNOWLEDGMENTS

C.G., V.N.F., and B.S.C. are senior researchers from the Brazilian National Research Council (CNPq) and acknowledge the financial support received during the development of this work from the Brazilian Research Agencies CAPES-PROCAD and Rede Nanobiotec, CNPq-INCT-Nano(Bio)Simes project 573925/2008-9, FAPERJ-CNPq (Pronex), CNPq project 478916/2010-8, National Institute of Science and Technology for Excitotoxicity and Neuroprotection – INCTEN, and FINEP Rede IBN 01.06.0842-00. E.W.S.C. received financial support from CNPq projects 304283/2010-0 and 474734/2011-0. The authors also thank Prof. David L. Azevedo, which kindly allowed us to use the DMOL3 code to carry out the DFT computations.

■ REFERENCES

- (1) Avram, S.; Duda-Seiman, D. M.; Svab, I.; Mancas, S.; Duda-Seiman, C.; Mihailescu, D. F. *Curr. Comput.-Aided Drug Des.* **2009**, *5*, 1.
- (2) Blobaum, A. L.; Marnett, L. J. *J. Med. Chem.* **2007**, *50*, 1425.
- (3) Vane, J. R.; Flower, R. J.; Botting, R. M. *Stroke* **1990**, *21*, IV12.
- (4) Gupta, K.; Selinsky, B. S.; Kaub, C. J.; Katz, A. K.; Loll, P. J. *J. Mol. Biol.* **2004**, *335*, 503.
- (5) Chandrasekharan, N. V.; Dai, H.; Roos, K. L.; Evanson, N. K.; Tomsik, J.; Elton, T. S.; Simmons, D. L. *Proc. Natl. Acad. Sci. U. S. A.* **2002**, *99*, 13926.
- (6) Schwab, J. M.; Beiter, T.; Linder, J. U.; Laufer, S.; Schulz, J. E.; Meyermann, R.; Schluesener, H. J. *FASEB J.* **2003**, *17*, 2174.
- (7) Vane, J. R.; Bakkle, Y. S.; Botting, R. M. *Annu. Rev. Pharmacol. Toxicol.* **1998**, *38*, 97.
- (8) Rao, P.; Knaus, E. E. *J. Pharm. Pharm. Sci.* **2008**, *11*, 81s.
- (9) Meade, E. A.; Smith, W. L.; DeWitt, D. L. *J. Biol. Chem.* **1993**, *268*, 6610.
- (10) Vane, J. R.; Botting, R. M. *Scand. J. Rheumatol.* **1996**, No. Suppl. 102, 9.
- (11) Vonkeman, H. E.; van de Laar, M. A. *Semin. Arthritis Rheum.* **2010**, *39*, 294.
- (12) Halen, P. K.; Murumkar, P. R.; Giridhar, R.; Yadav, M. R. *Mini Rev. Med. Chem.* **2009**, *9*, 124.
- (13) Smith, W. L.; Dewitt, D. L. *Adv. Immunol.* **1996**, *62*, 167.
- (14) Miyamoto, T.; Ogino, N.; Yamamoto, S.; Hayaishi, O. *J. Biol. Chem.* **1976**, *251*, 2629.
- (15) DeWitt, D. L.; Smith, W. L. *Proc. Natl. Acad. Sci. U. S. A.* **1988**, *85*, 1412.
- (16) Merlie, J. P.; Fagan, D.; Mudd, J.; Needleman, P. *J. Biol. Chem.* **1988**, *263*, 3550.
- (17) Yokoyama, C.; Takai, T.; Tanabe, T. *FEBS Lett.* **1988**, *231*, 347.
- (18) Loll, P. J.; Picot, D.; Garavito, R. M. *Nat. Struct. Biol.* **1995**, *2*, 637.
- (19) Picot, D.; Loll, P. J.; Garavito, R. M. *Nature* **1994**, *367*, 243.
- (20) Luong, C.; Miller, A.; Barnett, J.; Chow, J.; Ramesha, C.; Browner, M. F. *Nat. Struct. Biol.* **1996**, *3*, 927.

- (21) Kurumbail, R. G.; Stevens, A. M.; Gierse, J. K.; McDonald, J. J.; Stegeman, R. A.; Pak, J. Y.; Gildehaus, D.; Miyashiro, J. M.; Penning, T. D.; Seibert, K.; Isakson, P. C.; Stallings, W. C. *Nature* **1996**, *384*, 644.
- (22) Smith, W. L.; DeWitt, D. L.; Garavito, R. M. *Annu. Rev. Biochem.* **2000**, *69*, 145.
- (23) Vane, J. R. *Nat. New Biol.* **1971**, *231*, 232.
- (24) Ferreira, S. H.; Moncada, S.; Vane, J. R. *Nat. New Biol.* **1971**, *231*, 237.
- (25) Smith, J. B.; Willis, A. L. *Nat. New Biol.* **1971**, *231*, 235.
- (26) Wheatley, P. J. *J. Chem. Soc.* **1964**, 6036.
- (27) Filizola, M.; Perez, J. J.; Palomer, A.; Mauleon, D. *J. Mol. Graphics Modell.* **1997**, *15*, 290.
- (28) *Quantum Biochemistry*; Matta, C. F., Ed.; John Wiley & Sons, Inc.: London, 2010; Vol. 1.
- (29) Zhou, T.; Huang, D.; Caflisch, A. *Curr. Top. Med. Chem.* **2010**, *10*, 33.
- (30) Raha, K.; Peters, M. B.; Wang, B.; Yu, N.; Wollacott, A. M.; Westerhoff, L. M.; Merz, K. M. Jr. *Drug Discovery Today* **2007**, *12*, 725.
- (31) Ryde, U.; Nilsson, K. *J. Am. Chem. Soc.* **2003**, *125*, 14232.
- (32) Hohenberg, P.; Kohn, W. *Phys. Rev.* **1964**, *136*, B864.
- (33) Kohn, W.; Sham, L. J. *Phys. Rev.* **1965**, *140*, A1133.
- (34) Jorgensen, W. L. *Science* **2004**, *303*, 1813.
- (35) Hafner, J. *Nat. Mater.* **2010**, *9*, 690.
- (36) Lee, J. K.; Houk, K. N. *Science* **1997**, *276*, 942.
- (37) Zhang, D. W.; Zhang, J. Z. H. *J. Chem. Phys.* **2003**, *119*, 3599.
- (38) Zhang, D. W.; Xiang, Y.; Gao, A. M.; Zhang, J. Z. H. *J. Chem. Phys.* **2004**, *120*, 1145.
- (39) He, X.; Mei, Y.; Xiang, Y.; Zhang, D. W.; Zhang, J. Z. H. *Proteins: Struct., Funct., Bioinf.* **2005**, *61*, 423.
- (40) Zhang, Q. Y.; Wan, J.; Xu, X.; Yang, G. F.; Ren, Y. L.; Liu, J. J.; Wang, H.; Guo, Y. *J. Comb. Chem.* **2007**, *9*, 131.
- (41) Morozov, A. V.; Kortemme, T.; Tsemekhman, K.; Baker, D. A. V. *Proc. Natl. Acad. Sci. U. S. A.* **2004**, *101*, 6946.
- (42) Shen, J. W.; Zhang, J.; Luo, X. M.; Zhu, W. L.; Yu, K. Q.; Chen, K. X.; Li, Y. X.; Jiang, H. L. *Proc. Natl. Acad. Sci. U. S. A.* **2007**, *104*, 4337.
- (43) De Visser, S. P. *Biochem. Soc. Trans.* **2009**, *37*, 373.
- (44) Borowski, T.; de Marothy, S.; Broclawik, E.; Schofield, C. J.; Siegbahn, P. E. M. *Biochemistry* **2007**, *46*, 3682.
- (45) Plumley, J. A.; Dannenberg, J. J. *J. Am. Chem. Soc.* **2010**, *132*, 1758.
- (46) Liao, R. Z.; Yu, J. G.; Himo, F. *J. Phys. Chem. B* **2010**, *114*, 2533.
- (47) Favia, A. D.; Cavalli, A.; Masetti, M.; Carotti, A.; Recanatini, M. T. *Proteins* **2006**, *62*, 1074.
- (48) Cundari, T. R.; Wilson, A. K.; Drummond, M. L.; Gonzalez, H. E.; Jorgensen, K. R.; Payne, S.; Braunfeld, J.; De Jesus, M.; Johnson, V. M. *J. Chem. Inf. Model.* **2009**, *49*, 2111.
- (49) Yang, W. *Phys. Rev. A* **1991**, *44*, 7823.
- (50) Yang, W. T.; Lee, T. S. *J. Chem. Phys.* **1995**, *103*, 5674.
- (51) Gogonea, V.; Westerhoff, L. M.; Merz, K. M. *J. Chem. Phys.* **2000**, *113*, 5604.
- (52) Shaw, D. M.; St.-Amant, A. *J. Theor. Comput. Chem.* **2004**, *3*, 419.
- (53) Kobayashi, M.; Nakai, H. *Int. J. Quantum Chem.* **2009**, *109*, 2227.
- (54) Exner, T. E.; Mezey, P. G. *Phys. Chem. Chem. Phys.* **2005**, *7*, 4061.
- (55) He, X.; Zhang, J. Z. H. *J. Chem. Phys.* **2005**, *122*, 031103(1).
- (56) He, X.; Merz, K. M. Jr. *J. Chem. Theory Comput.* **2010**, *6*, 405.
- (57) Chen, X. H.; Zhang, D. W.; Zhang, J. Z. H. *J. Chem. Phys.* **2004**, *120*, 839.
- (58) Wu, E. L.; Mei, Y.; Han, K. L.; Zhang, J. Z. H. *Biophys. J.* **2007**, *92*, 4244.
- (59) Perdew, J. P.; Wang, Y. *Phys. Rev. Lett.* **1992**, *45*, 13244.
- (60) Perdew, J. P.; Burke, K.; Ernzerhof, M. *Phys. Rev. Lett.* **1996**, *77*, 3865.
- (61) Tkatchenko, A.; Scheffler, M. *Phys. Rev. Lett.* **2009**, *102*, 073005.
- (62) Zhao, Y.; Truhlar, D. G. *Phys. Chem. Chem. Phys.* **2005**, *7*, 2701.
- (63) van der Wijst, T.; Guerra, C. F.; Swart, M.; Bickelhaupt, F. M. *Chem. Phys. Lett.* **2006**, *426*, 415.
- (64) Cooper, V. R.; Thonhauser, T.; Langreth, D. C. *J. Chem. Phys.* **2008**, *128*, 204102.
- (65) Silvestrelli, P. L. *J. Phys. Chem. A* **2009**, *113*, 5224.
- (66) Ortmann, F.; Hannewald, K.; Bechstedt, F. *J. Phys. Chem. B* **2008**, *112*, 1540.
- (67) Ortmann, F.; Schmidt, W. G.; Bechstedt, F. *Phys. Rev. Lett.* **2005**, *95*, 186101.
- (68) Ortmann, F.; Bechstedt, F.; Schmidt, W. G. *Phys. Rev. B* **2006**, *73*, 205101.
- (69) Kee, E. A.; Livengood, M. C.; Carter, E. E.; McKenna, M.; Cafiero, M. *J. Phys. Chem. B* **2009**, *113*, 14810.
- (70) da Costa, R. F.; Freire, V. N.; Bezerra, E. M.; Cavada, B. S.; Caetano, E. W. S.; Filho, J. L. L.; Albuquerque, E. L. *Phys. Chem. Chem. Phys.* **2012**, *14*, 1389.
- (71) Hochgesang, G. P.; Rowlinson, S. W.; Marnett, L. J. T. *J. Am. Chem. Soc.* **2000**, *122*, 6514.
- (72) Ahmed, A.; Moman, E.; Adamo, M. F. A.; Nolan, K. B.; Chubb, A. *J. Bioorg. Med. Chem. Lett.* **2009**, *19*, 4213.